

Article

Vibrational Sum-Frequency Spectroscopic Investigation of the Structure and Azimuthal Anisotropy of Propynyl-Terminated Si(111) Surfaces

Purnim Dhar, Noah T Plymale, Sergey S. Malyk, Nathan S. Lewis, and Alexander V Benderskii

J. Phys. Chem. C, **Just Accepted Manuscript** • DOI: 10.1021/acs.jpcc.7b05256 • Publication Date (Web): 10 Jul 2017Downloaded from <http://pubs.acs.org> on July 10, 2017**Just Accepted**

“Just Accepted” manuscripts have been peer-reviewed and accepted for publication. They are posted online prior to technical editing, formatting for publication and author proofing. The American Chemical Society provides “Just Accepted” as a free service to the research community to expedite the dissemination of scientific material as soon as possible after acceptance. “Just Accepted” manuscripts appear in full in PDF format accompanied by an HTML abstract. “Just Accepted” manuscripts have been fully peer reviewed, but should not be considered the official version of record. They are accessible to all readers and citable by the Digital Object Identifier (DOI®). “Just Accepted” is an optional service offered to authors. Therefore, the “Just Accepted” Web site may not include all articles that will be published in the journal. After a manuscript is technically edited and formatted, it will be removed from the “Just Accepted” Web site and published as an ASAP article. Note that technical editing may introduce minor changes to the manuscript text and/or graphics which could affect content, and all legal disclaimers and ethical guidelines that apply to the journal pertain. ACS cannot be held responsible for errors or consequences arising from the use of information contained in these “Just Accepted” manuscripts.

1
2
3 **Vibrational Sum-Frequency Spectroscopic Investigation of the Structure and Azimuthal**
4 **Anisotropy of Propynyl-Terminated Si(111) Surfaces**
5
6

7 Purnim Dhar,[†] Noah T. Plymale,[‡] Sergey Malyk,[†] Nathan S. Lewis,[‡] and Alexander V.
8
9

10 Benderskii*[†]

11
12 [†]*Department of Chemistry, University of Southern California, Los Angeles, California 90089,*
13
14 *United States*

15
16
17 [‡]*Division of Chemistry and Chemical Engineering, Beckman Institute, and Kavli Nanoscience*
18
19 *Institute, California Institute of Technology, Pasadena, California 91125, United States*
20

21 **ABSTRACT**
22
23

24 Vibrational sum-frequency generation (VSFG) spectroscopy was used to investigate the
25 orientation and azimuthal anisotropy of the C–H stretching modes for propynyl-terminated
26 Si(111) surfaces, Si–C≡C–CH₃. VSFG spectra revealed symmetric and asymmetric C–H
27 stretching modes in addition to a Fermi resonance mode resulting from the interaction of the
28 asymmetric C–H bending overtone with the symmetric C–H stretching vibration. The
29 polarization dependence of the C–H stretching modes was consistent with the propynyl groups
30 oriented such that the Si–C≡C bond is normal to the Si(111) surface. The azimuthal angle
31 dependence of the resonant C–H stretching amplitude revealed no rotational anisotropy for the
32 symmetric C–H stretching mode and a 3-fold rotational anisotropy for the asymmetric C–H
33 stretching mode in registry with the 3-fold symmetric Si(111) substrate. The results are
34 consistent with expectation that the C–H stretching modes of a –CH₃ group are decoupled from
35 the Si substrate due to a –C≡C– spacer. In contrast, the methyl-terminated Si(111) surface, Si–
36 CH₃, was previously reported to have pronounced vibronic coupling of the methyl stretch modes
37 to the electronic bath of bulk Si. Vacuum-annealing of propynyl-terminated Si(111) resulted in
38 increased 3-fold azimuthal anisotropy for the symmetric stretch, suggesting that removal of
39
40
41
42
43
44
45
46
47
48
49
50
51
52
53
54
55
56
57
58
59
60

1
2
3 propynyl groups from the surface upon annealing allowed the remaining propynyl groups to tilt
4
5 away from the surface normal, into one of three preferred directions towards the vacated
6
7 neighbor sites.
8
9
10
11
12
13
14
15
16
17
18
19
20
21
22
23
24
25
26
27
28
29
30
31
32
33
34
35
36
37
38
39
40
41
42
43
44
45
46
47
48
49
50
51
52
53
54
55
56
57
58
59
60

I. INTRODUCTION

Chemical functionalization of inorganic semiconductor surfaces has been used to tune the interfacial dipole, relative band-edge positions, manipulate surface-state densities, improve chemical stability, and alter the optoelectronic properties of the resulting materials.¹⁻⁸ The orientation and conformation of chemisorbed or physisorbed molecules can contribute to the electronic coupling between the bound adsorbate and semiconductor material, thereby regulating on a molecular scale interfacial electron transfer, charge injection and extraction, charge transport, and electron tunneling at the interface.⁹⁻¹⁰ The energetics and coupling at the interface can be instrumental in controlling adsorbate-substrate energy transfer and in influencing reaction rates and mechanisms at the interface. A molecular-level understanding of functionalized semiconductor surfaces is thus necessary to elucidate interfacial chemistry and adsorbate-semiconductor interactions, which in turn can be used to inform device engineering.

Covalent attachment of organic moieties to oxide-free crystalline Si surfaces, while preserving the ideal electronic properties of H-terminated Si surfaces (H-Si(111)), would be an attractive route for the fabrication of highly passivated Si surfaces for applications in micro- and nanoelectronics,^{6, 11} photonics, solar-energy conversion,¹² and chemical and biological sensors.¹³⁻¹⁴ Methyl termination of Si(111) surfaces (CH₃-Si(111)) by a wet-chemical process yields atomically flat Si with all surface Si sites terminated.¹⁵⁻¹⁸ Although CH₃-Si(111) surfaces exhibit enhanced resistance to air oxidation compared to H-Si(111) surfaces,¹⁹⁻²⁰ -CH₃ groups are limited by a lack of methods to impart secondary functionalization.

Functionalization of the Si(111) surfaces with alkynyl moieties, such as ethynyl and propynyl groups, has the advantage of allowing for elaboration through the unsaturated -C≡C- units while still, in principle, maintaining nearly full Si-C surface termination.^{4, 21-24} Propynyl-

1
2
3 terminated Si(111) surfaces ($\text{CH}_3\text{CC-Si(111)}$) exhibit nearly complete termination of the Si(111)
4 surface while maintaining a relatively low, air-stable, surface recombination velocity.²⁴⁻³⁰
5
6 Previous characterization of $\text{CH}_3\text{CC-Si(111)}$ surfaces has also indicated that the $\text{CH}_3\text{CC-}$ groups
7
8 are oriented normal to the surface by infrared spectroscopy, the surfaces exhibit a (1×1) surface
9
10 unit cell by low-energy electron diffraction, and the surfaces exhibit broad atomic terraces by
11
12 atomic-force microscopy.²⁴ However, a full understanding of the chemical and electronic
13
14 structures of Si surfaces functionalized with alkynyl moieties is still lacking, owing to the
15
16 paucity of surface-sensitive spectroscopic techniques suitable for the detailed characterization of
17
18 molecular monolayers.
19
20
21
22
23

24
25 Vibrational sum-frequency-generation (VSFG) spectroscopy provides surface selectivity
26
27 and submonolayer sensitivity for in-situ investigations of the molecular structure and dynamics
28
29 at surfaces.³¹⁻³⁴ VSFG spectroscopy is a second-order nonlinear spectroscopic technique that,
30
31 under the electric dipole approximation, occurs only in the region of the material in which the
32
33 inversion symmetry is broken, specifically at the interface. The vibrational signatures of an
34
35 adsorbate in the mid-IR region are sensitive to the local environment, so VSFG spectroscopy can
36
37 be used in unraveling the adsorbate-adsorbate and adsorbate-substrate interactions.³⁵⁻⁴⁰ The input
38
39 and output beam polarizations of VSFG can be independently controlled to produce information
40
41 about the molecular orientation of the surface species.⁴¹
42
43
44
45

46
47 The molecular structure and rotational dynamics of $\text{CH}_3\text{-Si(111)}$ surfaces has been
48
49 elucidated using polarization-selected VSFG spectroscopy.⁴²⁻⁴³ The results indicated a strong
50
51 electronic interaction between the $-\text{CH}_3$ vibrational modes and the Si surface, but the extent to
52
53 which this coupling interaction is influenced by the proximity of the $-\text{CH}_3$ group to the Si(111)
54
55 surface has not been investigated. While both $\text{CH}_3\text{CC-Si(111)}$ and $\text{CH}_3\text{-Si(111)}$ surfaces have
56
57
58
59
60

1
2
3 vibrational signatures arising from $-\text{CH}_3$ groups, the distance between the $-\text{CH}_3$ groups and the
4 Si substrate is larger for $\text{CH}_3\text{CC}-\text{Si}(111)$ samples, allowing one to probe the dependence of
5 adsorbate-substrate interactions on the distance between the terminal $-\text{CH}_3$ group and the Si(111)
6 surface. The work reported herein describes a polarization-dependent VSFG study of the
7 propynyl-terminated Si(111) surface, to elucidate the surface structure and the adsorbate-
8 substrate interaction of this system.
9
10
11
12
13
14
15
16
17
18
19

20 II. EXPERIMENTAL

21
22 **II.A. Materials and Methods.** Water with a resistivity of $\geq 18.2 \text{ M}\Omega \text{ cm}$ was obtained
23 from a Barnstead E-Pure system. Ammonium fluoride ($\text{NH}_4\text{F}(\text{aq})$, 40%, semiconductor grade,
24 Transene Co., Inc., Danvers, MA) was purged with $\text{Ar}(\text{g})$ (99.999%, Air Liquide) for 1 h prior to
25 use. All other chemicals were used as received. Czochralski-grown n-type Si wafers (Virginia
26 Semiconductor, Fredericksburg, VA) were double-side polished, doped with phosphorus to a
27 resistivity of $1 \text{ }\Omega \text{ cm}$, $381 \pm 25 \text{ }\mu\text{m}$ thick, and oriented to within 0.1° of the (111) crystal plane.
28
29
30
31
32
33
34
35

36 *II.A.1. Preparation of H-Si(111) Surfaces.* The n-Si wafers were cut into $1 \text{ cm} \times 4 \text{ cm}$
37 pieces and rinsed sequentially with water, methanol ($\geq 99.8\%$, BDH), acetone ($\geq 99.5\%$, BDH),
38 methanol, and water. The wafers were oxidized and organic contaminants were removed by
39 immersing the wafers for 10 min in a piranha solution (1:3 v/v of 30% $\text{H}_2\text{O}_2(\text{aq})$ (EMD): 18 M
40 H_2SO_4 (EMD)) at $95 \text{ }^\circ\text{C}$. The wafers were removed and then rinsed with copious amounts of
41 water. The oxide was removed by immersing the wafers in buffered hydrofluoric acid ($\text{HF}(\text{aq})$,
42 Transene Co. Inc., Danvers, MA) for 18 s, rinsing with water, and immediately placing the
43 wafers for 9.0 min in an $\text{Ar}(\text{g})$ -purged solution of $\text{NH}_4\text{F}(\text{aq})$.^{24, 44-45} The wafers were agitated at
44
45
46
47
48
49
50
51
52
53
54
55
56
57
58
59
60

1
2
3 the start of each minute of etching, to remove bubbles that formed on the surface. The samples
4
5 were then removed from the etching solution, rinsed briefly with water, and dried under Ar(g).
6
7

8 *II.A.2. Preparation of Cl-Si(111) Surfaces.* The H-Si(111) samples were transferred to a
9
10 N₂(g)-purged glove box with <10 ppm O₂(g). An initiating amount (<1 mg mL⁻¹) of benzoyl
11
12 peroxide 98%, Sigma-Aldrich) was added to a saturated solution of PCl₅ (99.998% metal basis,
13
14 Alfa Aesar) in chlorobenzene (anhydrous, 99.8%, Sigma-Aldrich). The wafers were rinsed with
15
16 chlorobenzene and immersed in the PCl₅ solution at 90 ± 2 °C for 45 min.^{24, 45-46} The wafers
17
18 were removed from the reaction and rinsed with chlorobenzene followed by hexanes (anhydrous,
19
20 mixture of isomers, 99%, Sigma-Aldrich).
21
22
23

24 *II.A.3. Preparation of Propynyl-Terminated Si(111) Surfaces.* The Cl-Si(111) surfaces
25
26 were immersed in a 1.0 M solution of 1-propynyllithium (CH₃CCLi, BOC Sciences, Shirley,
27
28 NY) at 45 ± 2 °C for 15 h inside foil-wrapped test tubes. The wafers were removed from the
29
30 solution and rinsed with hexanes, followed by methanol (anhydrous, 99.8%, Sigma-Aldrich),
31
32 submerged in methanol, and removed from the glove box. The samples were sonicated for 10
33
34 min in methanol, rinsed with water, and dried under Ar(g). The samples were broken into 1 cm ×
35
36 1 cm squares, rinsed again with water, dried with Ar(g), and sealed under Ar(g) inside
37
38 polypropylene centrifuge tubes, to enable transport from Caltech to the University of Southern
39
40 California. X-ray photoelectron spectroscopy of the samples after preparation was consistent
41
42 with results reported previously,²⁴ indicating complete termination of the surface by CH₃CC-
43
44 groups and the absence of detectable levels of silicon oxide.
45
46
47
48
49

50 **II.B. VSFG Spectroscopy.** A detailed description of the VSFG apparatus can be found
51
52 elsewhere.⁴² In brief, the femtosecond mid-infrared and picosecond visible pulses used in the
53
54 broadband SFG spectroscopy setup were generated by splitting the 4 W output of a
55
56
57
58
59
60

1
2
3 regeneratively amplified Ti:sapphire laser system (Spectra Physics Spitfire seeded by a KM
4 Laboratories Oscillator) operating at 1 kHz repetition rate. The system delivered <100 fs pulses
5
6 centered at ~800 nm. An optical parametric amplifier assembly (TOPAS-C, Light Conversion)-
7
8 difference frequency generator (NDFG, Light Conversion) generated tunable femtosecond mid-
9
10 IR pulses (fwhm 350 cm^{-1}). The narrowband visible pulses were generated from the
11
12 uncompressed fundamental by passing the beam through an external compressor (Newport
13
14 Corporation) and an etalon (TecOptics, fwhm 17 cm^{-1}).
15
16
17
18
19

20 To generate the SFG signal, the IR and visible pulses were spatially and temporally
21 overlapped at the sample stage. SFG spectra were recorded using a triple-grating monochromator
22 in conjunction with a CCD cooled by liquid nitrogen. SFG spectra were collected under an
23 atmosphere of dry air obtained from a purge gas generator. To focus on the C–H stretching
24 region of the $\text{CH}_3\text{CC-Si}(111)$ samples, the IR pulse was centered at 3000 cm^{-1} . The beam was
25 focused on the sample using a 25 cm focal length CaF_2 lens for the IR beam and a 45 cm focal
26 length BK7 lens for the visible beam to yield a 200 μm diameter spot. The intensities of the
27 visible and the IR beams were 6–7 mW and 6–9 mW, respectively. Prior to VSFG
28 measurements, sample annealing was performed to remove surface impurities for 16–20 h under
29 ultrahigh vacuum at the temperatures ranging from 200–320 $^\circ\text{C}$ (see text).
30
31
32
33
34
35
36
37
38
39
40
41
42
43
44
45

46 **III. RESULTS**

47
48 **III.A. VSFG and Anisotropy Studies of $\text{CH}_3\text{CC-Si}(111)$ Surfaces.** Figure 1 presents
49 SFG spectra of the C–H stretching region for PPP (SFG-visible-IR) and SSP polarization
50 combinations, for as-prepared $\text{CH}_3\text{CC-Si}(111)$ samples at room temperature. A 270 fs time delay
51 between the IR and the visible pulses was used to collect both the PPP and the SSP spectra, to
52
53
54
55
56
57
58
59
60

suppress the nonresonant response of the silicon substrate.^{42-43, 47-48} The PPP spectrum showed three resonant vibrational modes of the terminal $-\text{CH}_3$ group, which are assignable to the symmetric C–H stretch (r^+) at $\sim 2865 \text{ cm}^{-1}$, the asymmetric C–H stretch (r^-) at $\sim 2962 \text{ cm}^{-1}$, and the Fermi resonance (d_{FR}^+) of the r^+ mode with the C–H asymmetric bending overtone, at $\sim 2933 \text{ cm}^{-1}$.^{24, 42, 49-51} The SSP spectrum, which exhibited a significant reduction in signal intensity compared with the PPP spectrum, only showed signatures ascribable to the symmetric C–H stretch (r^+) at $\sim 2863 \text{ cm}^{-1}$ and the Fermi resonance (d_{FR}^+) at $\sim 2935 \text{ cm}^{-1}$.

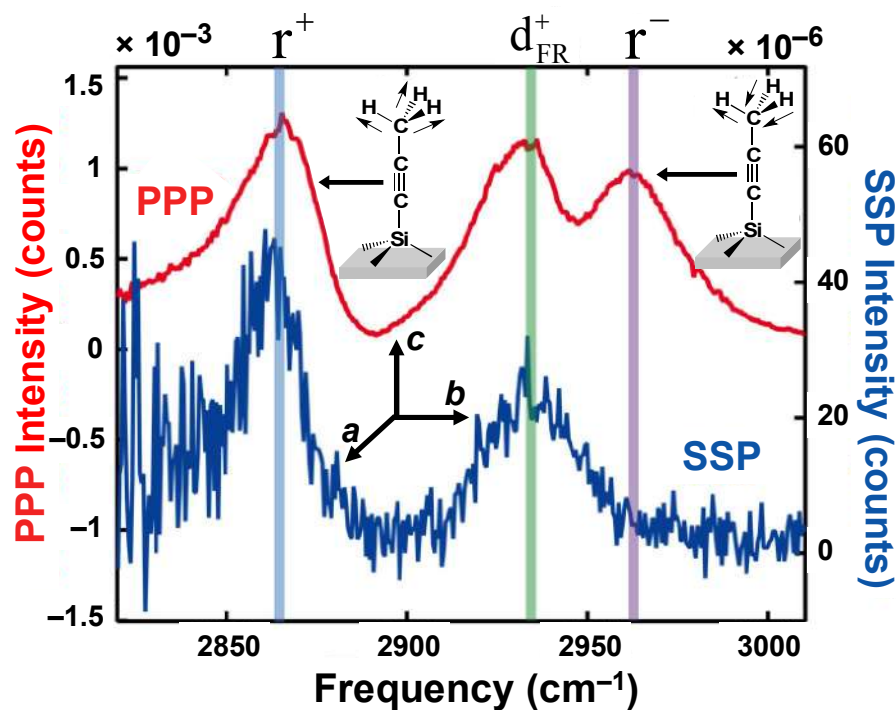


Figure 1. PPP (red, left axis) and SSP (blue, right axis) polarized VSG spectra of the $\text{CH}_3\text{CC}-\text{Si}(111)$ surface for the C–H stretching region. The time delay between the IR and the visible pulses was 270 fs. The corresponding molecular motions are shown alongside the VSG spectra. The molecular frame of reference (a, b, c) used in this work is indicated in the figure relative to the proposed orientation of the $\text{CH}_3\text{CC}-$ groups on the surface.

The azimuthal dependence of the resonant amplitudes of the r^+ and r^- modes of the $\text{CH}_3\text{CC-Si}(111)$ samples was measured^{42, 52-54} for azimuthal angles ϕ from 0° to 360° , and are shown for PPP polarization conditions in Figure 2. The data points represent the resonant C–H stretching mode amplitudes, which were obtained from the fits of the PPP spectra collected by in-plane rotation of the sample at 30° intervals (Table S2, Supporting Information). The polar plot for the r^+ mode (Figure 2A) showed only small changes in the amplitude of the resonant C–H stretching signal with ϕ , whereas the plot for the r^- mode showed a pronounced 3-fold dependence on the azimuthal angle (Figure 2B).

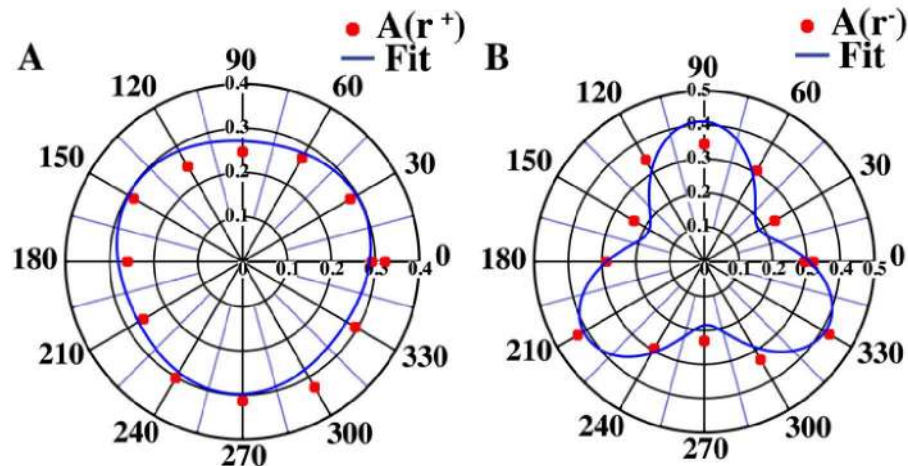
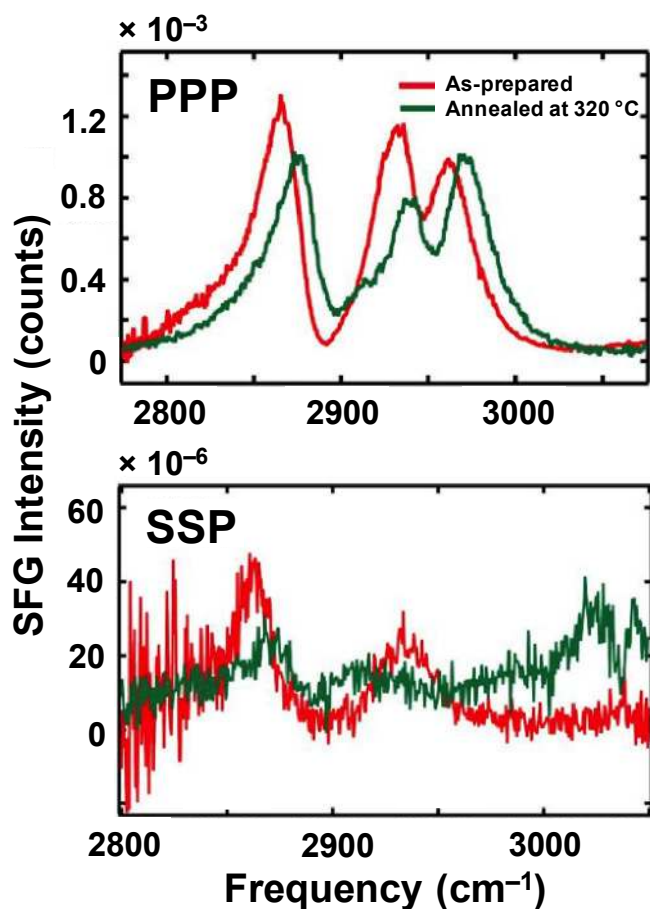


Figure 2. Polar plots showing the azimuthal dependence of the resonant amplitude of the C–H symmetric stretch r^+ (A) and C–H asymmetric stretch r^- (B), respectively, of the PPP spectra for as-prepared $\text{CH}_3\text{CC-Si}(111)$ samples. Data points were collected from 0° to 360° in 30° increments, and the blue solid lines are fits described in the text (Eq. (2)).

III.B. Effects of Annealing on the Adsorbate-Substrate Coupling Interaction. The stability of the $\text{CH}_3\text{CC-Si}(111)$ samples toward annealing in vacuum was investigated by VSFG spectroscopy. Samples were heated to $200\text{--}320^\circ\text{C}$ for $16\text{--}20$ h under vacuum, and were then

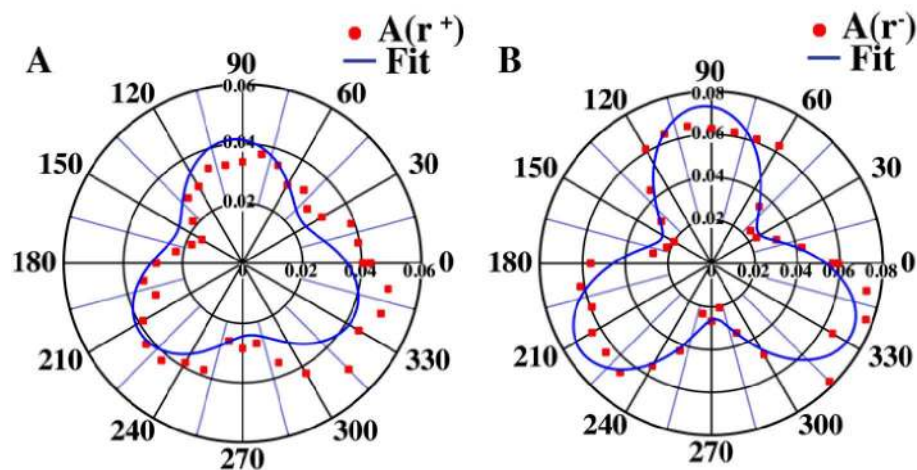
1
2
3 allowed to cool to room temperature for characterization by VSFG spectroscopy. The VSFG
4 spectra for the annealed samples (Figure 3) exhibited the same set of SFG transitions that were
5 seen for the as-prepared samples, with the r^+ and the d_{FR}^+ modes observed for both SSP and PPP
6 polarizations, and the r^- mode only observed for the PPP polarization. After annealing, the peak
7 intensities were reduced and the peak centers shifted by $\sim 5\text{--}9\text{ cm}^{-1}$ to higher energy relative to
8 the spectra obtained before annealing of the sample.
9
10
11
12
13
14
15
16
17



48
49
50
51
52
53
54
55
56
57
58
59
60

Figure 3. PPP and SSP spectra of the C–H stretching region of CH₃CC–Si(111) samples annealed at 320 °C for 16–20 h under vacuum. The decrease in intensity is consistent with the partial loss of the CH₃CC– units from the Si(111) surface upon annealing. The slight blue-shift of the peaks may be due to the changed local environment of the propynyl group remaining on the surface.

1
2
3
4
5
6 Figure 4 shows the dependence of the resonant amplitudes of the r^+ and r^- modes,
7
8 respectively, of the annealed $\text{CH}_3\text{CC-Si}(111)$ samples on the azimuthal angle ϕ for PPP
9
10 polarization conditions. The fits of the azimuthal rotational anisotropy data, collected for in-
11
12 plane rotation intervals of 10° (Table S3, Supporting Information), are shown superimposed on
13
14 the data points. After annealing, a 3-fold rotational anisotropy of the symmetric stretch r^+ mode
15
16 was readily observed, in contrast to the behavior prior to annealing. The 3-fold rotational
17
18 anisotropy exhibited by the r^- mode was slightly enhanced by the annealing step. The rotational
19
20 anisotropy of the resonant amplitudes of the r^+ and r^- modes was generally more pronounced
21
22 after annealing, indicating a change in the interaction between the $\text{CH}_3\text{CC-}$ adsorbates and the Si
23
24 substrate.
25
26
27
28
29



46
47
48
49
50
51
52
53
54
55
56
57
58
59
60

Figure 4. Polar plots showing the azimuthal dependence of the resonant amplitudes for PPP spectra of (A) the C–H symmetric stretch ($A(r^+)$) and (B) the C–H asymmetric stretch ($A(r^-)$) for $\text{CH}_3\text{CC-Si}(111)$ samples annealed at 200°C for 16–20 h under vacuum. Data points were collected from 0° to 360° in 10° increments, and the blue solid lines are fits described in the text (Eq. (2)).

IV. DISCUSSION

IV.A. VSFG Orientation Analysis of as-Prepared CH₃CC–Si(111) Samples. The sum frequency spectra of the CH₃CC–Si(111) samples were analyzed by macroscopic (ensemble) averaging of the resonant hyperpolarizability tensor elements ($\beta_{lmn}^{(2)}$, defined in the molecular frame (a, b, c)) that represent the methyl group vibrations (Figure 1).⁴¹ $\beta_{lmn}^{(2)}$ for the i -th vibrational mode is expressed as a product of the vibrational transition dipole moment and the Raman polarizability tensor:

$$\beta_{lmn,i}^{(2)} \propto \frac{\partial \alpha_{lm}}{\partial q_i} \frac{\partial \mu_n}{\partial q_i} \quad (1)$$

where q_i is the normal coordinate and the indices l, m , and n represent axes in the molecular frame of reference (a, b, c). Different vibrational modes have different symmetries, and the PPP and SSP polarization combinations sample different β tensor elements,⁵⁵⁻⁵⁷ which are also governed by the molecular symmetries. Hence, the absence of the r^- mode in the SSP spectrum provides a qualitative indication of the orientation of the CH₃CC– moieties perpendicular to the Si(111) surface.

The terminating CH₃CC– group can be approximately described as having C_{3v} symmetry, with c being the C₃ symmetry axis and the ac plane lying on one of the σ_v symmetry planes.^{55, 57} With respect to this molecule fixed coordinate system, the three C–H vibrational modes observed in the SFG spectra can be categorized into two different types of vibrations with different hyperpolarizability tensor elements.⁵⁸⁻⁵⁹ The r^+ and the d_{FR}^+ modes account for changes in the transition dipole moments along the c axis (perpendicular to the Si(111) surface plane), whereas the r^- mode accounts for changes along a direction that is perpendicular to the c axis (parallel to

1
2
3 the Si(111) surface plane). The corresponding β tensor elements for these modes can also be
4
5 categorized into two groups: the totally symmetric r^+ mode corresponds to two isotropic
6
7 independent β tensor elements, $\beta_{aac}^{(2)} = \beta_{bbc}^{(2)}$ and $\beta_{ccc}^{(2)}$, and the r^- mode corresponds to only one
8
9 independent β tensor element $\beta_{aca}^{(2)} = \beta_{caa}^{(2)}$.
10
11

12
13
14 With the symmetries of the β tensor elements for the r^+ and r^- modes taken into account,
15
16 along with knowledge of the input/output polarization combinations, the SSP spectra (which
17
18 sample tensor element $\chi_{yyz}^{(2)}$ defined in the laboratory frame of reference (x, y, z)) would contain
19
20 no peaks if the $\text{CH}_3\text{CC}-$ units were all oriented parallel to the Si(111) surface plane. In contrast,
21
22 if the $\text{CH}_3\text{CC}-$ units were all oriented perpendicular to the Si(111) surface plane, the SSP
23
24 spectrum would contain only peaks corresponding to vibrations perpendicular to the Si(111)
25
26 surface plane. Because the SSP spectra in Figures 1 and 3 exhibit signals ascribed to the r^+ and
27
28 d_{FR}^+ modes, the data are thus consistent with the $\text{CH}_3\text{CC}-$ groups being oriented perpendicular to
29
30 the Si(111) surface. The PPP spectra in Figure 1 and Figure 3 contain peaks corresponding to
31
32 both the parallel and perpendicular vibrations, as the spectrum is comprised of four different
33
34 susceptibility tensor elements ($\chi_{xxz}^{(2)}$, $\chi_{xzx}^{(2)}$, $\chi_{zxx}^{(2)}$, and $\chi_{xzz}^{(2)}$) sampling molecular
35
36 hyperpolarizabilities in all possible directions. The perpendicular orientation of the $\text{CH}_3\text{CC}-$
37
38 groups with respect to the Si(111) surface plane is consistent with the conclusions from variable-
39
40 angle transmission IR data on $\text{CH}_3\text{CC}-\text{Si}(111)$ samples.²⁴
41
42
43
44
45
46
47

48 **IV.B. Azimuthal Dependence of the Resonant C–H Stretch Amplitudes for as-**
49 **Prepared $\text{CH}_3\text{CC}-\text{Si}(111)$ Samples.** Both the adsorbate vibrational modes and the bulk Si
50
51 crystal polarizability contribute to the effective second-order vibrational response from the
52
53 functionalized Si(111) surface, as has been previously observed in VSFG studies of $\text{CH}_3-\text{Si}(111)$
54
55 surfaces.⁴² The coupling between the adsorbate vibrational modes and electronic bath of bulk Si
56
57
58
59
60

1
2
3 crystal, therefore, contributes to the azimuthal behavior of the resonant vibrational r^+ and r^-
4 modes for as-prepared $\text{CH}_3\text{CC-Si}(111)$ samples. Each of these contributions is comprised of an
5 isotropic component and an anisotropic component dependent on the crystal symmetry. For the
6 Si(111) surface, which has 3-fold rotational symmetry, the generated sum frequency field, E^{SFG} ,
7 has a form:
8
9

$$E^{\text{SFG}} = (A + C \cos(3\phi + \phi_0)) E^{\text{vis}} E^{\text{IR}} \quad (2)$$

10 where A and C are the isotropic and anisotropic contributions to the response, respectively, ϕ is
11 the azimuthal angle within the (111) plane with a phase correction of ϕ_0 , and E^{vis} and E^{IR} are the
12 input visible and mid-IR fields, respectively.
13
14

15 The observed azimuthal dependence of the VSFG signals can be connected to the
16 resonant vibrational modes via the unique β tensor elements that describe the $-\text{CH}_3$ group
17 vibrations. The non-zero β tensor elements for the r^+ mode are symmetric with respect to the C_3
18 axis ($\beta_{aac}^{(2)} = \beta_{bbc}^{(2)}$ and $\beta_{ccc}^{(2)}$) because the IR transition moment for the r^+ mode is along the C_3 axis
19 (which is along c), and the Raman polarizability tensor is isotropic about the symmetry axis.
20 Therefore, if the C_3 axis of the terminal $-\text{CH}_3$ group is normal to the surface, as evidenced by the
21 results reported herein, no azimuthal anisotropy for the r^+ mode is expected regardless of the in-
22 plane orientation of the $-\text{CH}_3$ group. The lack of clear rotational anisotropy for the r^+ mode
23 under PPP polarization conditions (Figure 2A) is consistent with this expectation. In contrast,
24 the β tensor elements for the r^- mode comprise the off-diagonal Raman polarizability tensor
25 elements ($\alpha_{ac} = \alpha_{ca}$), which are not symmetric about the C_3 axis. Further, the vibrational
26 transition dipole for the r^- mode is in-plane and also expected to be anisotropic, as long as the
27 molecules do not freely rotate in-plane. As a result, the r^- mode shows a 3-fold rotational
28 anisotropy (Figure 2B) that reflects the 3-fold symmetry of the crystalline Si(111) surface. The
29
30
31
32
33
34
35
36
37
38
39
40
41
42
43
44
45
46
47
48
49
50
51
52
53
54
55
56
57
58
59
60

1
2
3 3-fold anisotropy of the r^- mode also indicates that the $\text{CH}_3\text{CC}-$ groups do not rotate freely at
4 room temperature, but spend most of their time in one of the three energetic minima in registry
5 with the Si(111) surface, analogous to previously reported VSG results for $\text{CH}_3\text{-Si(111)}$
6 samples.⁴² This is additionally consistent with steric considerations on $\text{CH}_3\text{-Si(111)}$ or $\text{CH}_3\text{CC}-$
7 Si(111) surfaces that predict the interlocking of adjacent $-\text{CH}_3$ on the surface.^{18, 60} This
8 observation supports a close packing structure of the $\text{CH}_3\text{CC}-$ groups on the Si(111) surface,
9 suggesting that the surfaces are fully-terminated.

10
11
12
13
14
15
16
17
18
19
20 Previous VSG studies on the $\text{CH}_3\text{-Si(111)}$ surface showed a clear 3-fold azimuthal
21 anisotropy for the r^+ mode,⁴² in contrast to the results reported herein, which showed no such
22 anisotropy of the r^+ mode for as-prepared $\text{CH}_3\text{CC}-\text{Si(111)}$ samples. Because symmetry
23 considerations suggest that the r^+ mode should not exhibit rotational anisotropy, the results for
24 $\text{CH}_3\text{-Si(111)}$ surfaces were attributed to coupling between the adsorbate vibrational modes and
25 the above-band-gap Raman polarizability of the Si bulk.⁴² In the $\text{CH}_3\text{-Si(111)}$ system, the
26 coupling between the C-H vibrational modes and the electronic structure of the Si bulk is
27 strengthened by the close proximity of the $-\text{CH}_3$ group to the Si surface (the $-\text{CH}_3$ symmetric
28 stretch mode involves displacement of the carbon atom, and thus likely the attached Si atom).
29 Thus, the resultant Raman polarizability derivative for the $-\text{CH}_3$ group vibrations can be
30 expressed as:
31
32
33
34
35
36
37
38
39
40
41
42
43
44
45

$$\frac{\partial \alpha_{lm}}{\partial q_i} = \frac{\partial \alpha_{\text{Si}}}{\partial q_i} + \frac{\partial \alpha_{\text{Me}}}{\partial q_i} \quad (3)$$

46
47
48
49
50 where α_{Si} and α_{Me} are the electronic polarizability of the Si substrate and the $-\text{CH}_3$ group,
51 respectively. The polarizability scales with volume, so α_{Si} is expected to be much larger than α_{Me} ,
52 and the measured VSG signal is dominated by the above-band-gap electronic response of the Si
53 substrate. Hence the molecular hyperpolarizabilities for the $\text{CH}_3\text{-Si(111)}$ surface that correspond
54
55
56
57
58
59
60

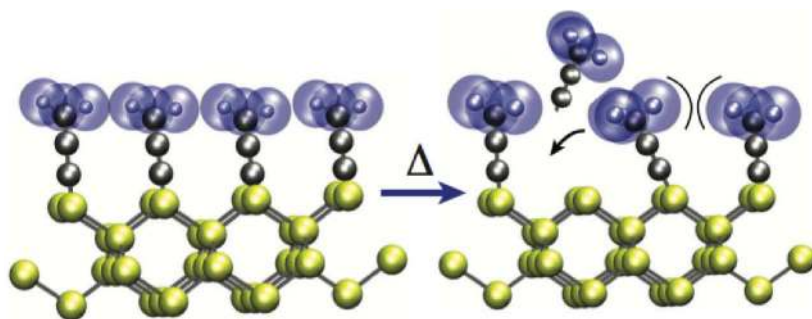
1
2
3 to the r^+ and r^- modes show the same 3-fold anisotropy of the Si(111) bulk regardless of the
4 orientations of their transition dipole moments with respect to the surface plane. The extent of
5 the adsorbate-substrate coupling decreases as the $-CH_3$ groups are further removed from the
6 Si(111) surface by the $-C\equiv C-$ spacer. The hyperpolarizability tensor elements for the r^+ mode
7 observed for $CH_3CC-Si(111)$ samples thus only reflect the totally symmetric Raman
8 polarizability tensor elements of the C-H symmetric vibrations of the methyl group uncoupled
9 from the Si substrate. The results reported herein suggest that the distance provided by the $-$
10 $C\equiv C-$ group is sufficient to substantially suppress the vibronic interaction between the $-CH_3$
11 group vibrations and the Si bulk.
12
13
14
15
16
17
18
19
20
21
22
23

24 **IV.C. Effects of Sample Annealing on the Structure of the $CH_3CC-Si(111)$ Surface.**

25
26 The azimuthal anisotropy of the r^+ and r^- modes for $CH_3CC-Si(111)$ was readily observed
27 following sample annealing to 200–320 °C (Figure 4). The appearance of an azimuthal
28 dependence for the r^+ mode and the increase in the observed anisotropy for the r^- mode can
29 potentially be attributed to the loss of CH_3CC- groups from the surface following annealing.
30 Previous thermal stability studies of $CH_3CC-Si(111)$ surfaces in vacuum have indicated loss of
31 CH_3CC- groups upon annealing to temperatures ≥ 200 °C, with ~ 0.76 ML remaining after
32 annealing for 30 min at 200 °C.²⁴ The decrease in SFG signal intensity of the C-H stretching
33 modes upon annealing in vacuum (Figure 3) supports the conclusion that CH_3CC- groups are
34 removed from the surface by this thermal process. The removal of a fraction of CH_3CC- units
35 results in vacancies on the Si(111) surface, which, in an otherwise closely packed structure,
36 could allow the remaining CH_3CC- groups adjacent to the defect sites to tilt away from the
37 surface normal. Thus, a propynyl molecule after annealing could tilt in one of the three
38
39
40
41
42
43
44
45
46
47
48
49
50
51
52
53
54
55
56
57
58
59
60

1
2
3 azimuthal directions towards its neighbors. Figure 5 depicts the proposed removal of a CH_3CC^-
4
5
6 unit by annealing and the subsequent reorganization of the surface structure.

7
8 As the direction of the C_3 symmetry axis of the CH_3CC^- group tilts away from the
9
10 surface normal, the β tensor elements for the r^+ mode will have resolvable components parallel to
11
12 the surface, and thus the SFG signal will exhibit 3-fold azimuthal anisotropy, as observed (Figure
13
14 4A). The observed decrease in SFG intensity is consistent with the partial loss of the CH_3CC^-
15
16 units from the Si(111) surface upon annealing, and with tilting of the molecular axis away from
17
18 surface normal. The tilt of the C_3 symmetry axis away from the surface normal also brings the
19
20 CH_3CC^- units closer to the Si surface, which may result in an increased coupling between the
21
22 CH_3CC^- units closer to the Si surface, which may result in an increased coupling between the
23
24 CH_3CC^- groups and the Si surface. The higher modulation depth of the r^- azimuthal response
25
26 (Figure 4B) is also consistent with this tilting.



43 **Figure 5.** Annealing causes loss of CH_3CC^- units from the Si(111) surface creating vacancy
44
45 defects. CH_3CC^- units adjacent to vacancies can tilt towards the Si(111) surface to relieve steric
46
47 strain. As CH_3CC^- units tilt toward the Si(111) surface plane, the terminal $-\text{CH}_3$ group acquires
48
49 in-plane component of the 2nd order susceptibility, thus resulting in the 3-fold anisotropy
50
51 observed in the VSDFG spectra.

52 53 54 55 56 57 **V. CONCLUSIONS**

1
2
3 The VSG studies of the CH₃CC–Si(111) surface emphasize the importance of the
4 molecular surface structure in determining the vibronic interactions between the semiconductor
5 bulk and the terminating substituents. The observation of only vibrational modes with transition
6 dipole moments oriented perpendicular to the surface plane for SSP polarization conditions
7 provides evidence that the CH₃CC– groups are oriented perpendicular to the surface. The
8 absence of azimuthal anisotropy observed for the r⁺ mode, in addition to the observed 3-fold
9 azimuthal anisotropy for the r⁻ mode, is consistent with expectations for C–H stretching
10 vibrations for a –CH₃ group is decoupled from the Si substrate due to the distance introduced by
11 the –C≡C– spacer group. This behavior stands in contrast to results observed for CH₃–Si(111)
12 surfaces, which showed significant electronic coupling between C–H vibrational modes and the
13 above-band-gap Raman polarizability of the Si bulk. The –C≡C– group present in CH₃CC–
14 Si(111) surfaces thus appears to effectively isolate the terminal –CH₃ group from the Si surface,
15 decoupling the C–H vibrational modes from the bulk electronic structure of the Si. Annealed
16 CH₃CC–Si(111) surfaces exhibited a more pronounced azimuthal anisotropy for the r⁺ and r⁻
17 modes compared with as-prepared samples. Loss of CH₃CC– groups from the surface upon
18 annealing and subsequent tilting of the remaining bound CH₃CC– groups towards the neighbor
19 vacancies and away from the surface normal results in the in-plane component of the
20 hyperpolarizability of the tilted –CH₃ group which leads to the observed 3-fold asymmetry.
21
22
23
24
25
26
27
28
29
30
31
32
33
34
35
36
37
38
39
40
41
42
43
44
45
46
47

48 ASSOCIATED CONTENT

49 Supporting Information

50 The supporting information is available free of charge on the ACS publications website at DOI:
51
52

53 Fitting parameters used to analyze the rotational anisotropy of the resonant amplitudes for PPP
54 spectra before and after annealing.
55
56
57
58
59
60

AUTHOR INFORMATION**Corresponding Author**

*(A.V.B.) E-mail: alex.benderskii@usc.edu. Tel: (213) 740-3220

Notes

The authors declare no competing financial interest.

ACKNOWLEDGMENTS

A.V.B. acknowledges the Air Force Office of Scientific Research under grant No. FA9550-15-1-0184. N.S.L. acknowledges the National Science Foundation under grant No. CHE-1214152. N.T.P. acknowledges support from a National Science Foundation Graduate Research Fellowship.

REFERENCES

1. Ashkenasy, G.; Cahen, D.; Cohen, R.; Shanzer, A.; Vilan, A., Molecular Engineering of Semiconductor Surfaces and Devices. *Accounts of Chemical Research* **2002**, *35*, 121-128.
2. Filler, M. A.; Bent, S. F., The Surface as Molecular Reagent: Organic Chemistry at the Semiconductor Interface. *Progress in Surface Science* **2003**, *73*, 1-56.
3. Loscutoff, P. W.; Bent, S. F., Reactivity of the Germanium Surface: Chemical Passivation and Functionalization. *Annu Rev Phys Chem* **2006**, *57*, 467-495.
4. Maldonado, S.; Plass, K. E.; Knapp, D.; Lewis, N. S., Electrical Properties of Junctions between Hg and Si(111) Surfaces Functionalized with Short-Chain Alkyls. *The Journal of Physical Chemistry C* **2007**, *111*, 17690-17699.
5. Seitz, O.; Vilan, A.; Cohen, H.; Hwang, J.; Haeming, M.; Schoell, A.; Umbach, E.; Kahn, A.; Cahen, D., Doping Molecular Monolayers: Effects on Electrical Transport through Alkyl Chains on Silicon. *Adv Funct Mater* **2008**, *18*, 2102-2113.

- 1
2
3
4
5
6
7
8
9
10
11
12
13
14
15
16
17
18
19
20
21
22
23
24
25
26
27
28
29
30
31
32
33
34
35
36
37
38
39
40
41
42
43
44
45
46
47
48
49
50
51
52
53
54
55
56
57
58
59
60
6. Vilan, A.; Yaffe, O.; Biller, A.; Salomon, A.; Kahn, A.; Cahen, D., Molecules on Si: Electronics with Chemistry. *Adv Mater* **2010**, *22*, 140-159.
 7. Li, Y.; O'Leary, L. E.; Lewis, N. S.; Galli, G., Combined Theoretical and Experimental Study of Band-Edge Control of Si through Surface Functionalization. *The Journal of Physical Chemistry C* **2013**, *117*, 5188-5194.
 8. Wong, K. T.; Lewis, N. S., What a Difference a Bond Makes: The Structural, Chemical, and Physical Properties of Methyl-Terminated Si(111) Surfaces. *Accounts of Chemical Research* **2014**, *47*, 3037-3044.
 9. Patitsas, S. N.; Lopinski, G. P.; Hul'ko, O.; Moffatt, D. J.; Wolkow, R. A., Current-Induced Organic Molecule–Silicon Bond Breaking: Consequences for Molecular Devices. *Surf Sci* **2000**, *457*, L425-L431.
 10. Tao, F. F.; Bernasek, S., *Functionalization of Semiconductor Surfaces*; John Wiley & Sons, Inc.: Hoboken, NJ, 2012.
 11. Chen, Y.; Wang, X.; Erramilli, S.; Mohanty, P.; Kalinowski, A., Silicon-Based Nanoelectronic Field-Effect Ph Sensor with Local Gate Control. *Appl Phys Lett* **2006**, *89*, 223512.
 12. Warren, E. L.; Atwater, H. A.; Lewis, N. S., Silicon Microwire Arrays for Solar Energy-Conversion Applications. *The Journal of Physical Chemistry C* **2014**, *118*, 747-759.
 13. Touahir, L., et al., Molecular Monolayers on Silicon as Substrates for Biosensors. *Bioelectrochemistry* **2010**, *80*, 17-25.
 14. Kirk, J. T.; Fridley, G. E.; Chamberlain, J. W.; Christensen, E. D.; Hochberg, M.; Ratner, D. M., Multiplexed Inkjet Functionalization of Silicon Photonic Biosensors. *Lab on a Chip* **2011**, *11*, 1372-1377.

- 1
2
3
4
5
6
7
8
9
10
11
12
13
14
15
16
17
18
19
20
21
22
23
24
25
26
27
28
29
30
31
32
33
34
35
36
37
38
39
40
41
42
43
44
45
46
47
48
49
50
51
52
53
54
55
56
57
58
59
60
15. Becker, J. S.; Brown, R. D.; Johansson, E.; Lewis, N. S.; Sibener, S. J., Helium Atom Diffraction Measurements of the Surface Structure and Vibrational Dynamics of $\text{CH}_3\text{-Si}(111)$ and $\text{Cd}_3\text{-Si}(111)$ Surfaces. *The Journal of Chemical Physics* **2010**, *133*, 104705.
16. Bansal, A.; Li, X.; Lauermann, I.; Lewis, N. S.; Yi, S. I.; Weinberg, W. H., Alkylation of Si Surfaces Using a Two-Step Halogenation/Grignard Route. *J Am Chem Soc* **1996**, *118*, 7225-7226.
17. Bansal, A.; Lewis, N. S., Stabilization of Si Photoanodes in Aqueous Electrolytes through Surface Alkylation. *The Journal of Physical Chemistry B* **1998**, *102*, 4058-4060.
18. Yu, H.; Webb, L. J.; Ries, R. S.; Solares, S. D.; Goddard, W. A.; Heath, J. R.; Lewis, N. S., Low-Temperature Stm Images of Methyl-Terminated Si(111) Surfaces. *The Journal of Physical Chemistry B* **2004**, *109*, 671-674.
19. Royea, W. J.; Juang, A.; Lewis, N. S., Preparation of Air-Stable, Low Recombination Velocity Si(111) Surfaces through Alkyl Termination. *Appl. Phys. Lett.* **2000**, *77*, 1988-1990.
20. Webb, L. J.; Lewis, N. S., Comparison of the Electrical Properties and Chemical Stability of Crystalline Silicon(111) Surfaces Alkylated Using Grignard Reagents or Olefins with Lewis Acid Catalysts. *J. Phys. Chem. B* **2003**, *107*, 5404-5412.
21. Teyssot, A.; Fidélis, A.; Fellah, S.; Ozanam, F.; Chazalviel, J. N., Anodic Grafting of Organic Groups on the Silicon Surface. *Electrochimica Acta* **2002**, *47*, 2565-2571.
22. Hurley, P. T.; Nemanick, E. J.; Brunschwig, B. S.; Lewis, N. S., Covalent Attachment of Acetylene and Methylacetylene Functionality to Si(111) Surfaces: Scaffolds for Organic Surface Functionalization While Retaining Si-C Passivation of Si(111) Surface Sites. *J Am Chem Soc* **2006**, *128*, 9990-9991.

- 1
2
3
4
5
6
7
8
9
10
11
12
13
14
15
16
17
18
19
20
21
22
23
24
25
26
27
28
29
30
31
32
33
34
35
36
37
38
39
40
41
42
43
44
45
46
47
48
49
50
51
52
53
54
55
56
57
58
59
60
23. Rohde, R. D.; Agnew, H. D.; Yeo, W.-S.; Bailey, R. C.; Heath, J. R., A Non-Oxidative Approach toward Chemically and Electrochemically Functionalizing Si(111). *J Am Chem Soc* **2006**, *128*, 9518-9525.
24. Plymale, N. T.; Kim, Y.-G.; Soriaga, M. P.; Brunschwig, B. S.; Lewis, N. S., Synthesis, Characterization, and Reactivity of Ethynyl- and Propynyl-Terminated Si(111) Surfaces. *The Journal of Physical Chemistry C* **2015**, *119*, 19847-19862.
25. Puniredd, S. R.; Assad, O.; Haick, H., Highly Stable Organic Modification of Si(111) Surfaces: Towards Reacting Si with Further Functionalities While Preserving the Desirable Chemical Properties of Full Si-C Atop Site Terminations. *J Am Chem Soc* **2008**, *130*, 9184-9185.
26. Bashouti, M. Y.; Sardashti, K.; Schmitt, S. W.; Pietsch, M.; Ristein, J.; Haick, H.; Christiansen, S. H., Oxide-Free Hybrid Silicon Nanowires: From Fundamentals to Applied Nanotechnology. *Progress in Surface Science* **2013**, *88*, 39-60.
27. Soria, F. A.; Paredes-Olivera, P.; Patrino, E. M., Chemical Stability toward O₂ and H₂O of Si(111) Grafted with -CH₃, -CH₂CH₂CH₃, -CHCH₃, and -CCH₃. *The Journal of Physical Chemistry C* **2015**, *119*, 284-295.
28. Puniredd, S. R.; Assad, O.; Haick, H., Highly Stable Organic Monolayers for Reacting Silicon with Further Functionalities: The Effect of the C-C Bond Nearest the Silicon Surface. *J Am Chem Soc* **2008**, *130*, 13727-13734.
29. Assad, O.; Puniredd, S. R.; Stelzner, T.; Christiansen, S.; Haick, H., Stable Scaffolds for Reacting Si Nanowires with Further Organic Functionalities While Preserving Si-C Passivation of Surface Sites. *J Am Chem Soc* **2008**, *130*, 17670-17671.

- 1
2
3
4
5
6
7
8
9
10
11
12
13
14
15
16
17
18
19
20
21
22
23
24
25
26
27
28
29
30
31
32
33
34
35
36
37
38
39
40
41
42
43
44
45
46
47
48
49
50
51
52
53
54
55
56
57
58
59
60
30. Qin, G.; Santos, C.; Zhang, W.; Li, Y.; Kumar, A.; Erasquin, U. J.; Liu, K.; Muradov, P.; Trautner, B. W.; Cai, C., Biofunctionalization on Alkylated Silicon Substrate Surfaces Via “Click” Chemistry. *J Am Chem Soc* **2010**, *132*, 16432-16441.
31. Zhu, X. D.; Suhr, H.; Shen, Y. R., Surface Vibrational Spectroscopy by Infrared-Visible Sum Frequency Generation. *Phys Rev B* **1987**, *35*, 3047-3050.
32. Richmond, G. L., Molecular Bonding and Interactions at Aqueous Surfaces as Probed by Vibrational Sum Frequency Spectroscopy. *Chem. Rev.* **2002**, *102*, 2693-2724.
33. Kim, J.; Somorjai, G. A., Molecular Packing of Lysozyme, Fibrinogen, and Bovine Serum Albumin on Hydrophilic and Hydrophobic Surfaces Studied by Infrared–Visible Sum Frequency Generation and Fluorescence Microscopy. *J Am Chem Soc* **2003**, *125*, 3150-3158.
34. Fu, L.; Liu, J.; Yan, E. C. Y., Chiral Sum Frequency Generation Spectroscopy for Characterizing Protein Secondary Structures at Interfaces. *J Am Chem Soc* **2011**, *133*, 8094-8097.
35. Guyot-Sionnest, P.; Dumas, P.; Chabal, Y. J.; Higashi, G. S., Lifetime of an Adsorbate-Substrate Vibration: H on Si(111). *Phys Rev Lett* **1990**, *64*, 2156-2159.
36. Lin, S. H.; Villaeys, A. A., Theoretical Description of Steady-State Sum-Frequency Generation in Molecular Adsorbates. *Phys Rev A* **1994**, *50*, 5134-5144.
37. Caudano, Y.; Silien, C.; Humbert, C.; Dreesen, L.; Mani, A. A.; Peremans, A.; Thiry, P. A., Electron–Phonon Couplings at C₆₀ Interfaces: A Case Study by Two-Color, Infrared–Visible Sum–Frequency Generation Spectroscopy. *Journal of Electron Spectroscopy and Related Phenomena* **2003**, *129*, 139-147.

- 1
2
3
4
5
6
7
8
9
10
11
12
13
14
15
16
17
18
19
20
21
22
23
24
25
26
27
28
29
30
31
32
33
34
35
36
37
38
39
40
41
42
43
44
45
46
47
48
49
50
51
52
53
54
55
56
57
58
59
60
38. Rupprechter, G.; Morkel, M.; Freund, H.-J.; Hirschl, R., Sum Frequency Generation and Density Functional Studies of Co–H Interaction and Hydrogen Bulk Dissolution on Pd(111). *Surf Sci* **2004**, *554*, 43-59.
39. Sovago, M.; Campen, R. K.; Wurpel, G. W. H.; Müller, M.; Bakker, H. J.; Bonn, M., Vibrational Response of Hydrogen-Bonded Interfacial Water Is Dominated by Intramolecular Coupling. *Phys Rev Lett* **2008**, *100*, 173901.
40. Stiopkin, I. V.; Weeraman, C.; Pieniazek, P. A.; Shalhout, F. Y.; Skinner, J. L.; Benderskii, A. V., Hydrogen Bonding at the Water Surface Revealed by Isotopic Dilution Spectroscopy. *Nature* **2011**, *474*, 192-195.
41. Wang, H.-F.; Velarde, L.; Gan, W.; Fu, L., Quantitative Sum-Frequency Generation Vibrational Spectroscopy of Molecular Surfaces and Interfaces: Lineshape, Polarization, and Orientation. *Annu Rev Phys Chem* **2015**, *66*, 189-216.
42. Malyk, S.; Shalhout, F. Y.; O’Leary, L. E.; Lewis, N. S.; Benderskii, A. V., Vibrational Sum Frequency Spectroscopic Investigation of the Azimuthal Anisotropy and Rotational Dynamics of Methyl-Terminated Silicon(111) Surfaces. *The Journal of Physical Chemistry C* **2012**, *117*, 935-944.
43. Shalhout, F. Y.; Malyk, S.; Benderskii, A. V., Relative Phase Change of Nearby Resonances in Temporally Delayed Sum Frequency Spectra. *J. Phys. Chem. Lett.* **2012**, *3*, 3493–3497.
44. Webb, L. J.; Rivillon, S.; Michalak, D. J.; Chabal, Y. J.; Lewis, N. S., Transmission Infrared Spectroscopy of Methyl- and Ethyl-Terminated Silicon(111) Surfaces. *J. Phys. Chem. B* **2006**, *110*, 7349-7356.

- 1
2
3
4 45. O'Leary, L. E.; Johansson, E.; Brunschwig, B. S.; Lewis, N. S., Synthesis and
5
6 Characterization of Mixed Methyl/Allyl Monolayers on Si(111). *The Journal of Physical*
7
8 *Chemistry B* **2010**, *114*, 14298-14302.
9
- 10 46. Rivillon, S.; Chabal, Y. J.; Webb, L. J.; Michalak, D. J.; Lewis, N. S.; Halls, M. D.;
11
12 Raghavachari, K., Chlorination of Hydrogen-Terminated Silicon (111) Surfaces. *Journal of*
13
14 *Vacuum Science and Technology A* **2005**, *23*, 1100-1106.
15
16
- 17 47. Lagutchev, A.; Hambir, S. A.; Dlott, D. D., Nonresonant Background Suppression in
18
19 Broadband Vibrational Sum-Frequency Generation Spectroscopy. *J. Phys. Chem. C* **2007**, *111*,
20
21 13645-13647.
22
23
- 24 48. Stiopkin, I. V.; Jayathilake, H. D.; Weeraman, C.; Benderskii, A. V., Temporal Effects on
25
26 Spectroscopic Line Shapes, Resolution, and Sensitivity of the Broad-Band Sum Frequency
27
28 Generation. *J. Chem. Phys.* **2010**, *132*, 234503.
29
30
- 31 49. Ferguson, G. A.; Raghavachari, K., Collective Vibrations in Cluster Models for
32
33 Semiconductor Surfaces: Vibrational Spectra of Acetylenyl and Methylacetylenyl Functionalized
34
35 Si(111). *The Journal of Chemical Physics* **2007**, *127*, 194706.
36
37
- 38 50. Yates, D. J. C.; Lucchesi, P. J., Infrared Spectra of Acetylene and Acetylene Derivatives
39
40 Adsorbed on Alumina and Silica. *The Journal of Chemical Physics* **1961**, *35*, 243-255.
41
42
- 43 51. Yang, F.; Hunger, R.; Roodenko, K.; Hinrichs, K.; Rademann, K.; Rappich, J.,
44
45 Vibrational and Electronic Characterization of Ethynyl Derivatives Grafted onto Hydrogenated
46
47 Si(111) Surfaces. *Langmuir* **2009**, *25*, 9313-9318.
48
49
- 50 52. Tom, H. W. K.; Heinz, T. F.; Shen, Y. R., Second-Harmonic Reflection from Silicon
51
52 Surfaces and Its Relation to Structural Symmetry. *Phys Rev Lett* **1983**, *51*, 1983-1986.
53
54
55
56
57
58
59
60

- 1
2
3
4
5
6
7
8
9
10
11
12
13
14
15
16
17
18
19
20
21
22
23
24
25
26
27
28
29
30
31
32
33
34
35
36
37
38
39
40
41
42
43
44
45
46
47
48
49
50
51
52
53
54
55
56
57
58
59
60
53. Sipe, J. E.; Moss, D. J.; van Driel, H. M., Phenomenological Theory of Optical Second- and Third-Harmonic Generation from Cubic Centrosymmetric Crystals. *Phys Rev B* **1987**, *35*, 1129-1141.
54. Mitchell, S. A.; Boukherroub, R.; Anderson, S., Second Harmonic Generation at Chemically Modified Si(111) Surfaces. *J. Phys. Chem. B* **2000**, *104*, 7668-7676.
55. Hirose, C.; Akamatsu, N.; Domen, K., Formulas for the Analysis of Surface Sum - Frequency Generation Spectrum by Ch Stretching Modes of Methyl and Methylene Groups. *The Journal of Chemical Physics* **1992**, *96*, 997-1004.
56. Hirose, C.; Yamamoto, H.; Akamatsu, N.; Domen, K., Orientation Analysis by Simulation of Vibrational Sum Frequency Generation Spectrum: Ch Stretching Bands of the Methyl Group. *The Journal of Physical Chemistry* **1993**, *97*, 10064-10069.
57. Wang, H.-F.; Gan, W.; Lu, R.; Rao, Y.; Wu, B.-H., Quantitative Spectral and Orientational Analysis in Surface Sum Frequency Generation Vibrational Spectroscopy (Sfg-Vs). *Int Rev Phys Chem* **2005**, *24*, 191-256.
58. Zhuang, X.; Miranda, P. B.; Kim, D.; Shen, Y. R., Mapping Molecular Orientation and Conformation at Interfaces by Surface Nonlinear Optics. *Phys Rev B* **1999**, *59*, 12632-12640.
59. Gautam, K. S.; Schwab, A. D.; Dhinojwala, A.; Zhang, D.; Dougal, S. M.; Yeganeh, M. S., Molecular Structure of Polystyrene at Air/Polymer and Solid/Polymer Interfaces. *Phys Rev Lett* **2000**, *85*, 3854-3857.
60. Nemanick, E. J.; Solares, S. D.; Goddard, W. A.; Lewis, N. S., Quantum Mechanics Calculations of the Thermodynamically Controlled Coverage and Structure of Alkyl Monolayers on Si(111) Surfaces. *The Journal of Physical Chemistry B* **2006**, *110*, 14842-14848.

1
2
3
4
5
6
7
8
9
10
11
12
13
14
15
16
17
18
19
20
21
22
23
24
25
26
27
28
29
30
31
32
33
34
35
36
37
38
39
40
41
42
43
44
45
46
47
48
49
50
51
52
53
54
55
56
57
58
59
60

TOC image

